

# IN SITU DENSITIES OF MORB MELTS AND RESIDUAL MANTLE: IMPLICATIONS FOR BUOYANCY FORCES BENEATH MID-OCEAN RIDGES<sup>1</sup>

YAOLING NIU AND RODEY BATIZA<sup>2</sup>

School of Ocean and Earth Sciences and Technology

## ABSTRACT

Recent theoretical studies of mid-ocean ridge (MOR) accretion have shown that the density differences between silicate melt and solid phases and between fertile and residual mantle may be important controls on the upward flow of upper mantle and separation of melt from the upwelling matrix. Both compositional and thermal buoyancy may play an important role. To assess quantitatively the magnitude of these effects, we have compiled the available data for calculating densities of silicate melts and solid phases as a function of composition, temperature (1000–1500°C), and pressure (1 atm to any pressure where the solid phases of interest remain stable). We include measured and calculated values of thermal expansion and compressibility for both solids and liquids. Our calculations for mantle material undergoing decompression-induced melting show that density differences between instantaneous melt and residual solids increase toward the surface, implying an increasing melt migration rate with continuing upwelling and melting. However, the density difference is significantly less than the value of  $\sim 0.5 \text{ g-cm}^{-3}$  commonly assumed in theoretical models. In agreement with previous studies, we also find that residual mantle is less dense than unmelted mantle; however, using realistic pressures for MORB generation, the difference is small.

## INTRODUCTION

Because of the geologic role of ocean crust in plate tectonic cycles, the processes that contribute to the formation of this crust are of great importance. An important aspect of the genesis of the mid-ocean ridge basalt (MORB) from which ocean crust is made is what causes hot solid mantle material to upwell beneath active spreading ridges. Upwelling may occur as a passive response to the separation of plates (Oxburgh and Turcotte 1968; Hanks 1971; Bottinga and Allègre 1978; Houseman 1983; Phipps Morgan 1987), and recent analysis of topography and gravity data (Lin and Phipps Morgan 1991) indicates that this may be the dominant mechanism beneath fast-spreading ridges. However, passive, two-dimensional upwelling of the upper mantle cannot explain all the observations, even at fast-spreading ridges. Along-axis topographic variation (Macdonald et al. 1984; Macdonald 1989), petrologic evidence (Langmuir et al. 1986), and model temperature profiles beneath mid-ocean ridges (Niu and Batiza 1991b) indicate that mantle upwelling is characterized by some three-dimensionality.

Another possible mechanism of mantle upwelling beneath active mid-ocean ridges is diapiric upflow. Gravity data at the slow-spreading mid-Atlantic ridge (Lin and Phipps Morgan 1991) suggest that such a mechanism may be important at slow-spreading ridges. Geologic evidence for diapiric flow has been found in ophiolites (Rabinowicz et al. 1987), and several theoretical models indicate that diapir-like instabilities may be important below mid-ocean ridges (Whitehead et al. 1984; Crane 1985; Schouten et al. 1985). These buoyant instabilities may be driven by thermal buoyancy, compositional buoyancy, or buoyancy provided by basalt melt (Oxburgh and Parmentier 1977; Jordan 1979). Buoyancy forces may thus play an important role in the generation of ocean crust. Many models of mid-ocean dynamics (e.g., Lachenbruch 1976; Ribe 1988; Nicolas 1986; Scott and Stevenson 1989; Buck and Su 1989; Sotin and Parmentier 1989) discuss the importance of buoyancy forces.

Density differences, along with other forces, are also important for melt migration and melt segregation below ridge crests (e.g., Ahearn and Turcotte 1979; McKenzie 1984, 1985; Spiegelman and McKenzie 1987; Richter and McKenzie 1984; Sleep 1974, 1988; Ribe 1985). Because of the great importance of melt and solid densities in the dynamic processes associated with the genesis of ocean crust, we have compiled up-to-date data on mineral densities and data needed to compute in situ densities at variable tempera-

<sup>1</sup> Manuscript received June 22, 1990; accepted April 22, 1991.

<sup>2</sup> University of Hawaii at Manoa, Honolulu, Hawaii, USA, 96822

[JOURNAL OF GEOLOGY, 1991, vol. 99, p. 767–775]  
© 1991 by The University of Chicago. All rights reserved.

0022-1376/91/9905-0025\$1.00

TABLE 1  
PARAMETERS USED TO CALCULATE MINERAL DENSITIES

Formula	Name	$\rho$ (g/cc)	$a$	$b$	$K_T^O$	$dK_T^O/dT$	$dK/dP$
		(25°C, 1 atm)	$\times 10^{-5}/^\circ\text{C}$	$\times 10^{-8}/^\circ\text{C}$	Kbar	Kbar/ $^\circ\text{C}$	(dimensionless)
<b>Olivine</b>							
Mg <sub>2</sub> SiO <sub>4</sub>	Forsterite	3.223(28)	- 10.353	- 1.9697(3,28,34)	1271(3,28,34)	- .239(3,28,34)	5.39(24)
Fe <sub>2</sub> SiO <sub>4</sub>	Fayalite	4.400(32)	- 12.124	- 2.2511(3,32,34)	1368(3,32,34)	- .268(3,32,34)	5.20(15)
<b>Orthopyroxene</b>							
Mg <sub>2</sub> Si <sub>2</sub> O <sub>6</sub>	Enstatite	3.204(8)	- 9.4732	- .0486(31)	1070(11,21,35)	- .270(14)	5.00(11)
Fe <sub>2</sub> Si <sub>2</sub> O <sub>6</sub>	Ferrosilite	4.003(8)	- 11.685	- .0826(31)	1010(7,24)	- .300(14)	5.00(11)
<b>Clinopyroxene</b>							
Mg <sub>2</sub> Si <sub>2</sub> O <sub>6</sub>	Clinoenstatite	3.206(8)	- 9.3865	- .0334(31)	1070†	- .270†	5.00†
Fe <sub>2</sub> Si <sub>2</sub> O <sub>6</sub>	Clinoferrosilite	4.005(29)	- 11.722	- .0686(31)	1010†	- .300†	5.00†
CaMgSi <sub>2</sub> O <sub>6</sub>	Diopside	3.272(23)	- 2.0119	- .1008(12)	1130(21)	- .200(1)*	4.50(26,27)
CaFeSi <sub>2</sub> O <sub>6</sub>	Hedenbergite	3.632(29)	- 2.2436	- .1003(31)	1200(21)	- .200(1)*	4.50(1)*
NaAlSi <sub>2</sub> O <sub>6</sub>	Jadeite	3.347(29)	- 8.7469	- .1803(10)	1430(21)	- .200(1)*	4.50(1)*
CaAl <sub>2</sub> SiO <sub>6</sub>	Ca-Tschermak	3.432(17)	- 7.7055	- 1.3155(17)	1200(1)*	- .200(1)*	5.00(1)*
<b>Garnet</b>							
Mg <sub>3</sub> Al <sub>2</sub> Si <sub>3</sub> O <sub>12</sub>	Pyrope	3.562(18)	- 8.7253	- .0474(31)	1750(18,25,30)	- .210(9)	4.50(25)
Fe <sub>3</sub> Al <sub>2</sub> Si <sub>3</sub> O <sub>12</sub>	Almandine	4.324(29)	- 9.9226	- .4912(31)	1779(5,30)	- .201(9)	5.45(36)
Ca <sub>3</sub> Al <sub>2</sub> Si <sub>3</sub> O <sub>12</sub>	Grossular	3.594(22)	- 8.1304	- .2493(31)	1700(18,25)	- .220(33)*	4.25(36)
Mn <sub>3</sub> Al <sub>2</sub> Si <sub>3</sub> O <sub>12</sub>	Spessartine	4.190(29)	- 11.113	- .3450(31)	1742(5,30)	- .220(33)*	4.59(36)
Ca <sub>3</sub> Fe <sub>2</sub> Si <sub>3</sub> O <sub>12</sub>	Andradite	3.860(29)	- 9.4224	- .0773(31)	1570(6)	- .220(33)*	5.00(1,11)*
Ca <sub>3</sub> Cr <sub>2</sub> Si <sub>3</sub> O <sub>12</sub>	Uvarovite	3.848(29)	- 9.3377	- .1233(31)	1620(6)	- .220(33)*	5.00(1,11)*
<b>Spinel</b>							
MgAl <sub>2</sub> O <sub>4</sub>	Spinel	3.577(29)	- 9.4271	- .1251(31)	1940(13)	- .220(1)*	4.00(13,37)
FeAl <sub>2</sub> O <sub>4</sub>	Hercynite	4.265(29)	- 9.8861	- .4143(31)	2103(37)	- .200(1)*	4.00(1,11)*
FeCr <sub>2</sub> O <sub>4</sub>	Chromite	5.086(29)	- 8.5401	- .1246(31)	2103(1)*	- .200(1)*	4.00(1,11)*
Fe <sub>2</sub> O <sub>4</sub>	Magnetite	5.201(29)	- 21.439	- .7541(31)	1860(13)	- .200(1)*	4.00(2,13)
MgCr <sub>2</sub> O <sub>4</sub>	Picrochromite	4.415(29)	- 7.5781	- 2.4431(31)	2100(1)*	- .200(1)*	4.00(1,11)*

TABLE 1  
(CONTINUED)

Plagioclase	Albite	2.611(29)	- 3.2612	- .8190(31,39)	699.3(4)	- .200(1)*	4.00(1)*
NaAlSi <sub>3</sub> O <sub>8</sub>							
CaAl <sub>2</sub> Si <sub>2</sub> O <sub>8</sub>	Anorthite	2.762(29)	- 1.6459	- 1.3693(16,31)	943.4(4)	- .200(1)*	4.00(1)*

† No data for clinoenstatite and clinoferrosilite are available, but those of enstatite and ferrosilite are used instead (see text for discussion).  
\* No data or no consistent data available, the values are assumed (see text for discussion)  
References: 1) Anderson (1989); 2) Anderson and Anderson (1970); 3) Anderson and Suzuki (1983); 4) Angel et al (1988); 5) Babusaka et al (1978); 6) Bass (1986); 7) Bass and Weidner (1984); 8) Berman (1988); 9) Bonczar et al (1977); 10) Cameron et al (1973); 11) Duffy and Anderson (1989); 12) Finger and Ohashi (1976); 13) Finger et al (1986); 14) Frisillo and Barsch (1972); 15) Graham et al (1988); 16) Grundy and Brown (1974); 17) Haselton et al (1984); 18) Hazen and Finger (1978); 19) Hazen and Prewitt (1977); 20) Isaak and Graham (1976); 21) Kandelin and Weidner (1988); 22) Krupka et al (1979); 23) Krupka et al (1985); 24) Kuwazawa and Anderson (1969); 25) Leitner et al (1980); 26) Levien and Prewitt (1981); 27) Levien et al (1979); 28) Matsui and Manghani (1985); 29) Robie et al (1967); 30) Sato et al (1978); 31) Skinner (1966); 32) Suzuki et al (1981); 33) Suzuki et al (1983a); 34) Suzuki et al (1983b); 35) Vaughan and Bass (1983); 36) Wang and Simmons (1974); 37) Wang and Simmons (1972); 38) Weaver et al (1976); 39) Winter et al (1979);

tures and pressures in the melting range of peridotite for MORB. We also discuss briefly how these latter data are used to calculate densities and to present some results of such calculations. Our new compilation and methodology allow rapid calculations of in situ density for melts and solids as a function of temperature, pressure, and composition.

## METHODS

Melt densities are calculated as a function of temperature, pressure, and composition by the method of Lange and Carmichael (1987) in combination with thermal expansion data for MnO of Bottinga et al. (1982).

For solid minerals, we evaluate the temperature dependence of density for individual end-member components as follows:

$$\rho(T, 1 \text{ bar}) = \rho_{25^\circ\text{C}}^0 + a(T-25) + b(T-25)^2 \quad (1)$$

Ideal mixing of end-member components (table 1) is assumed in dealing with the temperature effect on densities of solid solutions. We neglect the pressure effect on thermal expansion, following Lange and Carmichael (1987) and Herzberg (1987a, 1987b). This is reasonable since this effect on calculated densities is of the order of  $10^{-6}$  for the pressure range of interest. The pressure effect is given by the well-known third-order Birch-Murnaghan equation of state:

$$P = \frac{3}{2} K_T \left[ R^{7/3} - R^{5/3} \right] \cdot \left[ 1 + \frac{3}{4} (4 - K') (R^{2/3} - 1) \right] \quad (2)$$

where  $K_T$  is the isothermal bulk modulus at the temperature of interest and atmospheric pressure, which is calculated by  $K_T = K_T^0 + dK_T^0/dT(T - T_R)$ ;  $K'$  is the pressure derivative of  $K_T^0$ ,  $dK_T^0/dP$ ; and  $R = V(T,1)/V(T,P) = \rho(T,P)/\rho(T,1)$ . We compute  $\rho(T,P)$  by successive approximation of the pressure calculated with equation 2 to the pressure of interest. A computer program that uses the data of table 1 to calculate in situ densities of solid mantle compositions and melts is given in Niu and Batizu (1991a) and is available from the authors.

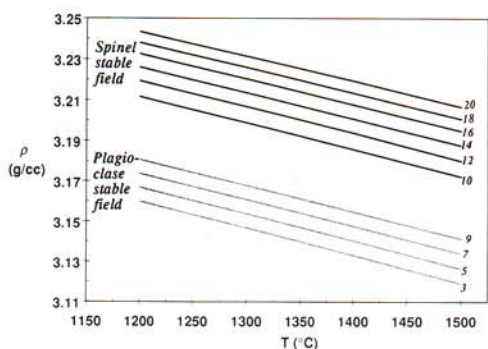


FIG. 1.—Calculated densities of a fertile mantle (MPY-90 of Falloon and Green 1987) to show the effect of temperature and pressure alone without considering compositional effects due to melting for the pressure range of interest in MORB genesis. Numerals to the right are pressures in kilobars. The temperature effect on densities of the fertile mantle is only about  $0.013$  to  $0.014$   $\text{g}\cdot\text{cm}^{-3}/100^\circ\text{C}$ . The pressure (depth) effect is also small, on the order of  $0.032$   $\text{g}\cdot\text{cm}^{-3}/10$  kb for both spinel- and plagioclase-peridotite fields. Including phase changes, however, the overall pressure effect on mantle densities in the melting range of peridotite beneath mid-ocean ridges may be as much as  $0.05$   $\text{g}\cdot\text{cm}^{-3}/10$  kb.

#### APPLICATION TO BUOYANCY BELOW ACTIVE MID-OCEAN RIDGES

Using the data of table 1 and equations 1 and 2, densities of mantle material may be calculated. Elsewhere (Niu and Batiza 1991*b*) we show that decompression-induced melting to produce most natural MORB compositions begins at pressures of about 10 to 22 kbars. In this study, we confine ourselves to this pressure range, which is well within the spinel and plagioclase stability fields, consistent with studies of abyssal oceanic peridotite (Dick et al. 1984). Figure 1 shows the density variation of a solid fertile mantle (MPY-90 of Falloon and Green 1987) as a function of temperature and pressure. It is clear from this figure that thermal buoyancy in solid mantle is only  $0.013$ – $0.014$   $\text{g}\cdot\text{cm}^{-3}/100^\circ\text{C}$ . The pressure (depth) effect is on the order of  $0.032$   $\text{g}\cdot\text{cm}^{-3}/10$  kb for both the spinel- and plagioclase-peridotite fields; however a dramatic density change accompanies the spinel/plagioclase phase transition, which we arbitrarily set at 9 kb. If the phase change is included, the overall pressure effect on melt-free solid mantle densities relevant to MORB genesis may be up to  $0.05$   $\text{g}\cdot\text{cm}^{-3}/10$  kb.

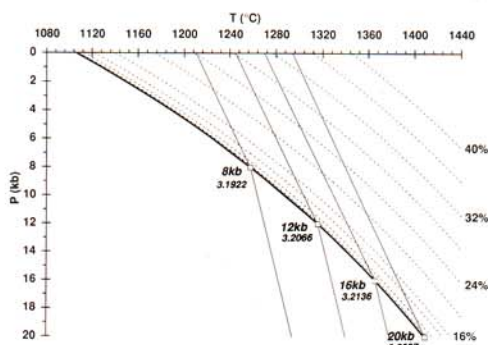


FIG. 2.—Adiabatic melting paths of upwelling mantle in  $P$ - $T$  space. Thick solid line and thin dashed lines are mantle (MPY-90) solidus and isopleths of extent of partial melting (Niu and Batiza 1991*b*). Thin solid lines are adiabatic upwelling paths adopted from McKenzie (1984). Pressure values (20 kb, 16 kb, 12 kb, and 8 kb) indicate the initial melting pressures along melting paths that cross the solidus. Values in italics are the densities of unmelted mantle at the indicated  $P$ - $T$  points (open squares).

Compositional buoyancy due to melt extraction may also be important (Oxburgh and Parmentier 1977; Jordan 1979; Buck and Su 1989; Sotin and Parmentier 1989). We use the adiabatic upwelling melting model of Niu and Batiza (1991*b*) to evaluate this effect. This model calculates major element compositions of MORB melts using solid-liquid partition coefficients ( $D_i$ ) empirically derived from peridotite melting experiments (Jaques and Green 1980; Falloon et al. 1988; Falloon and Green 1987, 1988). We empirically determine  $D_i = f(P, T)$  and use this to calculate melt compositions. For column melting initiated by decompression, we assume rapid removal of melt from the solid matrix (McKenzie 1984, 1985*b*). We start by producing a 4% batch melt of a given peridotite. After that, with continued upwelling, melt is produced in incremental 1% batches and removed. The residue of each increment is calculated by mass balance and becomes the source for the next melt increment. We calculate both instantaneous and pooled melt compositions, and calculate the mineralogy and mode of the residue using a modified CIPW norm calculation combined with a least-squares procedure that gives results in good agreement with experimental data and modal data for abyssal peridotite (Dick et al. 1984). For more details of the melting model, see Niu and Batiza

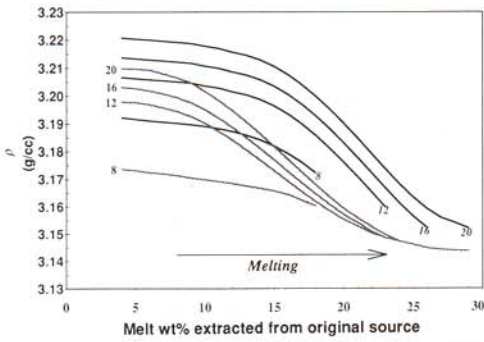


FIG. 3.—Calculated densities of residual solids (stippled lines) as melting proceeds. Numerals to the left are the pressures (in kilobars) of initial melting along the four adiabatic paths (fig. 2 shows how the extent of melt extracted is related to pressure release along the melting paths). For comparison, the densities of solid fertile mantle (no melting) are plotted as solid lines. Solid mantle density values are computed for  $P$ - $T$  conditions shown in figure 2. Numerals to the lower right are corresponding initial melting pressures along these paths. This comparison explicitly displays the density reduction of solid mantle due to melt extraction. The largest density reduction is only about  $0.040 \text{ g}\cdot\text{cm}^{-3}$ , and for most conditions, the effect is only  $0.015\text{--}0.025 \text{ g}\cdot\text{cm}^{-3}$ . There are several uncertainties in calculating the densities of solid mantle materials (fertile or residual peridotite). The most important source of error is uncertainty in calculating the mineralogy and mode of the solid assemblages. We estimate these errors on the order of  $\pm 0.01\text{--}0.03 \text{ g}\cdot\text{cm}^{-3}$ . Uncertainties in the relative differences in density, however, such as those shown in this figure, are probably much smaller.

(1991*b*). Figure 2 shows the adiabatic melting paths of Niu and Batiza (1991*b*), which we use in this study.

Figure 3 shows the effect of melt extraction on the density of solid (melt-free) residual mantle. For the scenarios we consider, the density differences between fertile mantle (solid lines) and residual mantle (stippled lines) are smaller than estimated in the literature (e.g., Buck and Su [1989] estimate a density difference of  $0.10 \text{ g}\cdot\text{cm}^{-3}$  with 30% melt extraction and Sotin and Parmentier [1989] estimate a density difference of  $\sim 0.06 \text{ g}\cdot\text{cm}^{-3}$  for 20% melt extraction). Figure 3 shows a maximum density difference of  $0.035\text{--}0.040 \text{ g}\cdot\text{cm}^{-3}$  with values of  $0.015\text{--}0.025 \text{ g}\cdot\text{cm}^{-3}$  for most reasonable conditions. Considering the uncertainties of our model, which primarily arise from uncertainties in the mineralogy and mode of fertile and residual solids (discussed later), a value of  $0.06 \text{ g}\cdot\text{cm}^{-3}$  (Sotin

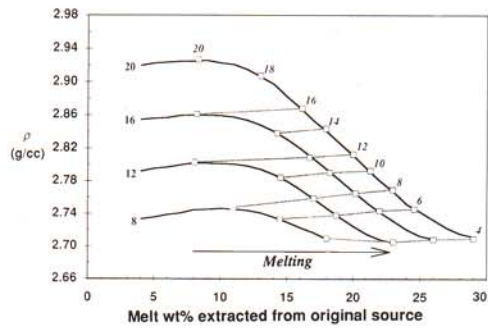


FIG. 4.—Calculated densities (thick solid lines) of instantaneous MORB melt produced as melting proceeds along the four adiabatic melting paths (initial melting pressures in kilobar labeled to the left; see fig. 2 for changing  $P$  and  $T$  conditions). The compositions of the instantaneous melt as a function of  $P$ ,  $T$ , and extent of melt extraction are calculated using the method of Niu and Batiza (1991*b*). For an upwelling mantle parcel, melting occurs first as a 4% batch melt. Thereafter, melting occurs as 1% increments by batch melting; however the melt is removed from the residue. Thus the residue left after each increment of melting becomes the source for the next increment. Melt compositions are computed using bulk solid-melt distribution coefficients for the major elements. The coefficients were determined from laboratory experiments and are corrected for temperature and pressure effects (see Niu and Batiza 1991*b*). The stippled lines are isobars (in kilobars, labeled to the right) to show the compositional and temperature effect on instantaneous melt densities.

and Parmentier 1989) probably represents an extreme. Thus compositional buoyancy due to melt extraction, while larger than the effect of thermal expansion or compressibility alone (fig. 1), is rather small in the spinel or plagioclase peridotite field. Despite the small absolute value of this effect, if compositional and thermal buoyancy are dynamically balanced (see, e.g., Sotin and Parmentier 1989; Scott and Stevenson 1989), time-dependent episodic behavior of mantle upwelling can result.

Figure 4 shows the density of instantaneous column melts produced as a function of the total melt extracted along the melting paths (fig. 2). These calculated in situ melt densities include the effects of composition (Niu and Batiza 1991*b*), thermal expansion, and compressibility. Figure 5 compares the density of the instantaneous melt in a given increment of melting with the density of the coexisting solid residue. Because of the greater compressibility of melt (Stolper et al.

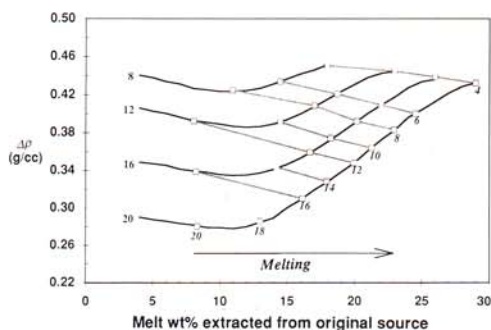


FIG. 5.—Density differences (solid thick lines) between instantaneous MORB melt (see fig. 4) and solid residues (see stippled lines in fig. 3) as melting proceeds along the four adiabatic paths (see fig. 2). The stippled lines are isobars as in figure 4. This clearly shows that the density differences between the melt and residue vary from  $0.28 \text{ g-cm}^{-3}$  to  $0.45 \text{ g-cm}^{-3}$ , and increase with decreasing pressure. See caption to figure 3 for uncertainties in the densities of solid residues and text for discussion.

1981; Lange and Carmichael 1987; Agee and Walker 1988)  $\Delta\rho$  ( $\rho_{\text{residue}} - \rho_{\text{melt}}$ ) decreases with increasing in situ pressure. As upwelling and melting proceed, the  $\Delta\rho$  values increase. This effect is rather large (see fig. 5) and could modify the results of Scott and Stevenson (1989), who assumed a greater, and pressure-independent,  $\Delta\rho$  of  $0.5 \text{ g-cm}^{-3}$ , possibly too high by a factor of two.

Melt retention in the mantle is another potential source of buoyancy beneath mid-ocean ridges (Scott and Stevenson 1989). The density of porous mantle residue containing melt can be computed easily; however the amount of melt retention in upwelling mantle below ridges is presently controversial. The effect of 1–3% melt is of the order  $\sim 1$  to  $\sim 5 \times 10^{-3} \text{ g-cm}^{-3}$  in reducing the density of the bulk mantle.

#### DISCUSSION AND CONCLUSIONS

Our method provides for rapid and accurate calculations of thermal and compositional buoyancy of melts and solid phases. Errors in calculated densities of melts and solid minerals using equations 1 and 2 and our data compilation are expected to be

small, on the order of  $5 \times 10^{-4}$  to  $\sim 5 \times 10^{-3} \text{ g-cm}^{-3}$ , because measurement errors in the original studies are on this order. However, additional errors stem from uncertainties in estimating the modes of solid phases and their compositions. These uncertainties are difficult to evaluate with our present knowledge. Given possible uncertainties of up to 10% in the relative modal proportion of major mantle minerals (olivine, orthopyroxene, and clinopyroxene, for example), the calculated densities for solid mantle may be subject to errors of up to  $\pm 0.01$  to  $0.03 \text{ g-cm}^{-3}$ . These uncertainties will not affect our main conclusions, since they are based on relative density differences between fertile mantle and residual mantle (fig. 3). For calculated density differences between residual solids and in situ melt (fig. 5), the uncertainties may be greater (up to  $0.04 \text{ g-cm}^{-3}$ ) but cannot now be estimated with confidence.

One conclusion of this study is that the effect of the presence of melt on the density of mantle residue plus melt increases greatly with decreasing pressure, as expected. Our main conclusion is that the density difference between melt and solid residue is generally smaller than assumed in theoretical studies of buoyancy-driven mantle flow, which has important implications for buoyancy below ridges.

ACKNOWLEDGMENTS.—We gratefully acknowledge financial support for this study from the NSF (OCE 89-03296 and OCE-90-00193) and the ONR. Discussions with J. Phipps Morgan, R. Buck, D. Scott, M. Spiegelman, C. Sotin, J. Lin, Y. Chen, W. Su, C. Langmuir, B. White, H. Dick, P. Michael, T. Grove, R. Kinzler and many other 1990 Ridge Summer Institute participants have been very helpful. We particularly thank J. Phipps Morgan, J. Lin, Y. Chen, and W. Su for their constructive comments on an earlier draft of this paper. The formal reviews of A. Philpotts and several anonymous reviewers greatly improved an earlier version of the paper. University of Hawaii, School of Ocean and Earth Sciences and Technology contribution: 2425.

#### REFERENCES CITED

- AGEE, G. B., and WALKER, D., 1988, Static compression and olivine floatation in ultrasonic silicate liquid: *Jour. Geophys. Res.*, v. 93, p. 3437–3449.
- AHEARN, J. L., and TURCOTTE, D. L., 1979, Magma migration beneath an ocean ridge: *Earth Planet. Sci. Res. Lett.*, v. 45, p. 115–122.
- ANDERSON, D. L., 1989, *Theory of the Earth*: London, Blackwell Scientific, 366 p.
- , and ANDERSON, O. L., 1970, The bulk mod-

- ulus volume relationship for oxides: *Jour. Geophys. Res.*, v. 75, p. 3494–3500.
- ANDERSON, O. L., and SUZUKI, I., 1983, Anharmonicity of three minerals at high temperature: forsterite, fayalite, and periclase: *Jour. Geophys. Res.*, v. 88, p. 3549–3556.
- ANGEL, R. J.; HAZEN, R. M.; McCORMICK, T. C.; PREWITT, C. T.; and SMYTH, J. R., 1988, Comparative compressibility of end-member feldspars: *Phys. Chem. Minerals*, v. 15, p. 313–318.
- BABUSKA, V.; FIALA, J.; KUMAZAWA, M.; OHNO, I.; and SUMINO, Y., 1978, Elastic properties of garnet solid solution series: *Phys. Earth Planet. Inter.*, v. 16, p. 157–176.
- BASS, J. D., 1986, Elasticity of uvarovite and andradite garnets: *Jour. Geophys. Res.*, v. 91, p. 7505–7516.
- , and WEIDNER, D. J., 1984, Elasticity of single-crystal orthopyroxene: *Jour. Geophys. Res.*, v. 89, p. 4359–4371.
- BERMAN, G., 1988, Internally consistent thermodynamic data for mineral system  $\text{Na}_2\text{O-K}_2\text{O-CaO-MgO-FeO-Fe}_2\text{O}_3\text{-Al}_2\text{O}_3\text{-SiO}_2\text{-TiO}_2\text{-H}_2\text{O-CO}_2$ : *Jour. Petrol.*, v. 29, p. 445–552.
- BONCZAR, L. J.; GRAHAM, E. K.; and WANG, H., 1977, The pressure and temperature dependence of the elastic constants of pyrope garnet: *Jour. Geophys. Res.*, v. 82, p. 2529–2534.
- BOTTINGA, Y., and ALLÈGRE, C. J., 1978, Partial melting under spreading ridges: *Royal Soc. (London) Philos. Trans.*, v. 288 A, p. 501–525.
- ; WEILL, D.; and RICHTER, P., 1982, Density calculations for silicate liquids. I. Revised method for aluminosilicate compositions: *Geochim. Cosmochim. Acta*, v. 46, p. 909–919.
- BUCK, W. R., and SU, W., 1989, Focused mantle upwelling below mid-ocean ridges due to feedback between viscosity and melting: *Geophys. Res. Lett.*, v. 16, p. 641–644.
- CAMERON, M.; SUENO, S.; PREWITT, C. T.; and PAPIKE, J. J., 1973, High-temperature crystal chemistry of acmite, diopside, hedenbergite, jadeite, spondumene, and ureyite: *Am. Mineral.*, v. 58, p. 594–618.
- CRANE, K., 1985, The spacing of rift-axis highs: dependence upon diapiric processes in the underlying asthenosphere?: *Earth Planet. Sci. Lett.*, v. 72, p. 405–414.
- DICK, H. J. B.; FISHER, R. L.; and BRYAN, E. B., 1984, Mineralogical variability of the uppermost mantle along mid-ocean ridges: *Earth Planet. Sci. Lett.*, v. 69, p. 88–106.
- DUFFY, T. S., and ANDERSON, D., 1989, Seismic velocities in mantle minerals and the mineralogy of upper mantle: *Jour. Geophys. Res.*, v. 94, p. 1895–1912.
- FALLOON, T. J., and GREEN, D. H., 1987, Anhydrous partial melting of MORB pyrolite and other peridotite compositions at 10 kbar: implications for the origin of MORB glasses: *Mineral. Petrol.*, v. 37, p. 181–219.
- , and ———, 1988, Anhydrous partial melting of peridotite from 8 to 35 kb and the petrogenesis of MORB: *Jour. Petrol.*, Special Lithosphere Issue, p. 379–414.
- ; ———; HATTON, C. J.; and HARRIS, K. L., 1988, Anhydrous partial melting of a fertile and depleted peridotite from 2 to 30 kb and application to basalt petrogenesis: *Jour. Petrol.*, v. 29, p. 1257–1282.
- FINGER, L. W.; HAZEN, R. M.; and HOFMEISTER, A. M., 1986, High-pressure crystal chemistry of spinel ( $\text{MgAl}_2\text{O}_4$ ) and magnetite ( $\text{Fe}_3\text{O}_4$ ): comparisons with silicate spinels: *Phys. Chem. Minerals*, v. 13, p. 215–220.
- , and OHASHI, Y., 1976, The thermal expansion of diopside to 800°C and a refinement of crystal structure at 700°C: *Am. Mineral.*, v. 61, p. 303–310.
- FRISILLO, A. L., and BARSCH, A. L., 1972, Measurement of single-crystal constants of bronzite as a function of pressure and temperature: *Jour. Geophys. Res.*, v. 77, p. 6360–6384.
- GRAHAM, E. K.; SCHWAB, J. A.; SOKPIN, S. M.; and TAKEI, H., 1988, The pressure and temperature dependence of the elastic properties of single-crystal fayalite  $\text{Fe}_2\text{SiO}_4$ : *Phys. Chem. Minerals*, v. 16, p. 186–198.
- GRUNDY, H. D., and BROWN, W. L., 1974, A high temperature X-ray study of low and high plagioclase feldspars, in MACKENZIE, W. S., and ZUSSMAN, J., eds., *The Feldspar*, Proceedings of a NATO Adv. Study Inst.: University of Manchester Press, p. 162–173.
- HANKS, T. C., 1971, Model relating heat-flow values near and vertical velocities of mass transport beneath ocean rises: *Jour. Geophys. Res.*, v. 76, p. 537–544.
- HASELTON, H. T., JR.; HEMINGWAY, B. S.; and ROBIE, R. A., 1984, Low-temperature heat capacities of  $\text{CaAl}_2\text{SiO}_6$  glass and pyroxene and thermal expansion of  $\text{CaAl}_2\text{SiO}_6$  pyroxene: *Am. Mineral.*, v. 69, p. 481–489.
- HAZEN, R. M., and FINGER, L. W., 1978, Crystal structure and compressibilities of pyrope and grossular to 60 kbar: *Am. Mineral.*, v. 63, p. 297–303.
- , and PREWITT, C. T., 1977, Linear compressibilities of low albite: high-pressure structural implications: *Am. Mineral.*, v. 62, p. 554–558.
- HERZBERG, C., 1987a, Magma density at high pressure. Part 1: the effect of composition on the elastic properties of silicate liquids, in MYSEN, B. O., ed., *Magmatic processes: physical chemical principles*: *Geochem. Soc. Spec. Pub.*, v. 1, p. 25–46.
- , 1987b, Magma density at high pressure. Part 2: a test of the olivine floatation hypothesis, in MYSEN, B. O., ed., *Magmatic processes: physical chemical principles*: *Geochem. Soc. Spec. Pub.*, v. 1, p. 47–58.
- HOUSEMAN, G., 1983, The deep structure of ocean ridges in a convecting mantle: *Earth Planet. Sci. Lett.*, v. 64, p. 283–294.
- ISAAK, D. G., and GRAHAM, E. K., 1976, The elastic properties of an almandine-spessartine garnet and elasticity in the garnet solid solution series: *Jour. Geophys. Res.*, v. 81, p. 2483–2489.
- JAQUES, A. L., and GREEN, D. H., 1980, Anhydrous melting of peridotite at 0–15 kb pressure and the genesis of tholeiitic basalts: *Contrib. Mineral. Petrol.*, v. 73, p. 287–310.
- JORDAN, T. H., 1979, Mineralogies, densities, and

- seismic velocities of garnet lherzolites and their geophysical implications, in *BOYD, F. R., and MEYER, H. O., eds., Proc. Second Int. Kimberlite Conf., v. 2, p. 1-14.*
- KANDELIN, J., and WEINDER, D. J., 1988, Elastic properties of hedenbergite: *Jour. Geophys. Res., v. 93, p. 1063-1072.*
- KRUPKA, K. M.; ROBIE, R. A.; and HEMINGWAY, B. S., 1979, High-temperature heat capacities of corundum, periclase, anorthite,  $\text{CaAl}_2\text{Si}_2\text{O}_8$  glass, muscovite, pyrophyllite,  $\text{KAlSi}_3\text{O}_8$  glass, grossular, and  $\text{NaAlSi}_3\text{O}_8$  glass: *Am. Mineral., v. 64, p. 86-101.*
- ; ———; ———; KERRICK, D. M.; and ITO, J., 1985, Low-temperature heat capacities and derived thermodynamic properties of anthophyllite, diopside, enstatite, bronzite, and wallstonite: *Am. Mineral., v. 70, p. 249-260.*
- KUWASAWA, M.; and ANDERSON, O. L., 1969, Elastic moduli, pressure derivatives, and temperature derivatives of single-crystal olivine and single-crystal forsterite: *Jour. Geophys. Res., v. 74, p. 5961-5972.*
- LACHENBRUCH, A. H., 1976, Dynamics of a passive spreading centers: *Jour. Geophys. Res., v. 81, p. 1883-1902.*
- LANGE, R. A., and CARMICHAEL, I. S. E., 1987, Densities of  $\text{Na}_2\text{O-K}_2\text{O-CaO-MgO-FeO-Fe}_2\text{O}_3\text{-Al}_2\text{O}_3\text{-TiO}_2\text{-SiO}_2$  liquids: new measurements and derived partial molar properties: *Geochem. Cosm. Acta, v. 51, p. 2931-2946.*
- LANGMUIR, C. H.; BENDER, J. F.; and BATIZA, R., 1986, Petrological and tectonic signatures of the East Pacific Rise  $5^\circ30'N-14^\circ30'N$ : *Nature, v. 322, p. 422-429.*
- LEITNER, B. J.; WEIDNER, D. J.; and LIEBERMANN, R. C., 1980, Elasticity of single crystal pyrope and implications for garnet solid solution series: *Phys. Earth Planet. Inter., v. 22, p. 111-121.*
- LEVIEN, L., and PREWITT, C. T., 1981, High pressure structural study of diopside: *Am. Mineral., v. 66, p. 315-323.*
- ; WEIDNER, D. J.; and PREWITT, C., 1979, Elasticity of diopside: *Phys. Chem. Minerals, v. 4, p. 105-113.*
- LIN, J., and PHIPPS MORGAN, J., 1990, The spreading rate dependence of three-dimensional mid-ocean ridge gravity structure: *Geophys. Res. Lett., in press.*
- MACDONALD, K. C., 1989, Tectonic and magmatic processes on the East Pacific Rise, in *The Geology of North America, v. N, The Eastern Pacific Ocean and Hawaii: Geol. Soc. America, p. 93-110.*
- ; SEMPERE, J.-C.; and FOX, P. J., 1984, East Pacific Rise from Siqueiros to Orozco fracture zones: along strike continuity of axial neovolcanic zones and structure and evolution of overlapping spreading centers: *Jour. Geophys. Res., v. 89, p. 6049-6069.*
- MATSUI, T., and MANGHNANI, M. H., 1985, Thermal expansion of single-crystal forsterite to 1023 K by Fizeau interferometry: *Phys. Chem. Minerals, v. 12, p. 201-210.*
- McKENZIE, D., 1984, The generation and compaction of partially molten rock: *Jour. Petrol., v. 25, p. 713-765.*
- , 1985, The extraction of magma from the crust and mantle: *Earth Planet. Sci. Lett., v. 79, p. 81-91.*
- NICOLAS, A., 1986, A melt extraction model based on structural studies in mantle peridotites: *Jour. Petrol., v. 27, p. 999-1022.*
- NIU, Y., and BATIZA, R., 1991a, DENSCAL: a program for calculating densities of silicate melts and mantle minerals in melting range: *Computers and Geosciences, in press.*
- , and ———, 1991b, An empirical methods for calculating melt compositions produced beneath mid-ocean ridges: application for axis and off-axis (seamounts) melting: *Jour. Geophys. Res., in press.*
- OXBURGH, E. R., and PARMENTIER, E. M., 1977, Compositional and density stratification in the oceanic lithosphere—causes and consequences: *Jour. Geol. Soc. London, v. 133, p. 343-354.*
- , and TURCOTTE, D. L., 1968, mid-ocean ridge and geotherm distribution during mantle convection: *Jour. Geophys. Res., v. 73, p. 26-43.*
- PHIPPS MORGAN, J., 1987, Melt migration beneath mid-ocean ridge spreading centers: *Geophys. Res. Lett., v. 14, p. 1238-1241.*
- RABINOWICZ, M.; CEULENEER, G.; and NICOLAS, A., 1987, Melt segregation and flow in mantle diapirs below spreading centers: evidence from Oman ophiolite: *Jour. Geophys. Res., v. 92, p. 3475-3486.*
- RIBE, N. M., 1985, The deformation and compaction of partially molten zones: *Geophys. Jour. Royal Astron. Soc., v. 83, p. 487-501.*
- , 1988, On the dynamics of mid-ocean ridges: *Jour. Geophys. Res., v. 93, p. 429-436.*
- RICHTER, F. M., and MCKENZIE, D. P., 1984, Dynamical models for melt segregation from a deformable matrix: *Jour. Geol., v. 92, p. 729-740.*
- ROBIE, R. A.; BETHKE, P. M.; and BEARDSLEY, K. M., 1967, Selected X-ray crystallographic data, molar volumes, and densities of minerals and related substances: *U.S. Geol. Survey Bull. 1248, 87 p.*
- SATO, Y.; AKAOGI, M.; and AKIMOTO, S.-I., 1978, Hydrostatic compression of the synthetic garnet pyrope and almandine: *Jour. Geophys. Res., v. 83, p. 335-338.*
- SCOTT, D. R., and STEVENSON, D. J., 1989, A self-consistent model of melting, magma migration, and buoyancy-driven circulation beneath mid-ocean ridges: *Jour. Geophys. Res., v. 94, p. 2973-2988.*
- SCHOUTEN, H.; KLITGORD, K. D.; and WHITEHEAD, J. A., 1985, Segmentation of mid-ocean ridges: *Nature, v. 317, p. 225-229.*
- SKINNER, B. J., 1966, Thermal expansion. Handbook of physical constants: *Geol. Soc. America Mem. 97, p. 75-96.*
- SLEEP, N. H., 1974, segregation of magma from a mostly crystalline mush: *Geol. Soc. America Bull., v. 85, p. 1225-1232.*
- SLEEP, N. H., 1988, Tapping of magmas from ubiq-



- uitous mantle heterogeneities: an alternative to mantle plumes?: *Jour. Geophys. Res.*, v. 93, p. 10,255-10,272.
- SOTIN, C., and PARMENTIER, E. M., 1989, Dynamic consequences of compositional and thermal density stratification beneath spreading centers: *Geophys. Res. Lett.*, v. 16, p. 835-838.
- SPIEGELMAN, M., and MCKENZIE, D., 1987, Simple 2-D models for melt extraction at mid-ocean ridges and island arcs: *Earth Planet. Sci. Lett.*, v. 83, p. 137-152.
- STOLPER, E.; WALKER, D.; HAGER, B. H.; and HAYS, J. F., 1981, Melt segregation from partially molten source region: the importance of melt density and source region size: *Jour. Geophys. Res.*, v. 86, p. 6261-6271.
- SUZUKI, I., and ANDERSON, O. L., 1983a, Elasticity and thermal expansion of a natural garnet up to 1,000 K: *Jour. Phys. Earth*, v. 31, p. 125-138.
- ; ———; and SUMINO, Y., 1983b, Elastic properties of a single-crystal forsterite  $Mg_2SiO_4$ , up to 1200 K: *Phys. Chem. Minerals*, v. 10, p. 38-46.
- ; SEYOSHI, K.; TAKEI, H.; and SUMINO, Y., 1981, Thermal expansion of Fayalite,  $Fe_2SiO_4$ : *Phys. Chem. Minerals*, v. 7, p. 60-63.
- VAUGHAN, M. T., and BASS, J. D., 1983, Single-crystal elastic properties of protoenstatite: a comparison with orthoenstatite: *Phys. Chem. Minerals*, v. 10, p. 62-68.
- WANG, H., and SIMMONS, G., 1972, Elasticity of some mantle crystal structures 1. Pleonaste and hercynite spinel: *Jour. Geophys. Res.*, v. 77, p. 4379-4392.
- , and ———, 1974, Elasticity of some mantle crystal structures 3. Spessartine-almondine garnet: *Jour. Geophys. Res.*, v. 79, p. 2607-2613.
- WEAVER, J. S.; TAKAHASHI, T.; and BASS, J. 1976, Isothermal compression of grossular garnets to 250 Kbar and the effect of calcium on the bulk modulus: *Jour. Geophys. Res.*, v. 81, p. 2474-2482.
- WHITEHEAD, J. A.; DICK, H. J. B.; and SCHOUTEN, H., 1984, A mechanism for magmatic accretion under spreading centers: *Nature*, v. 312, p. 146-147.
- WINTER, J. K.; OKAMURA, F. P.; and GHOSE, S., 1979, A high-temperature structural study of high albite, monalbite, and albite-monalbite phase transition: *Am. Mineral.*, v. 64, p. 409-423.